I (14):
II (20):
III (16):

Schriftliche Prüfung aus Grundlagen der Digitalen Bildverarbeitung WS 2009/2010

Walter G. Kropatsch

Bitte tragen Sie Ihre Matrikelnummer, Ihren Namen und Ihre Studienkennzahl in die dafür vorgesehenen Kästchen ein:

Grundlagen der Digitalen Bildverarbeitung LV 183.126		Datum: 7.12.2010
Mat.Nr.	Name	Studium

Diese Prüfung besteht aus drei Teilen auf die Sie insgesamt 50 Punkte erreichen können. Für besonders gute Begründungen können Zusatzpunkte erreicht werden. Die Dauer der Prüfung beträgt 90 Minuten. Es gilt der folgende Notenschlüssel:

Note:	1	2	3	4	5
Punkte:	> 42	37:42	31:36	25:30	0:24

Teil I: Interpretation von Bildoperationen (14)

Im ersten Teiles sollen Sie Ergebnisbilder über vorgegebene Operationen mit den gegebenen Eingabebildern in Beziehung setzen. Auf den folgenden 2 Seiten finden Sie 24 Bilder die als Eingabe als auch als Ergebnis einer Bildoperation auftreten können. Beachten Sie, dass nicht ALLE Bilder verwendet werden, es kann Bilder geben, die nicht als Eingabe- oder Ergebnisbilder aufscheinen.

Allgemeines

Die angegebenen Bilder haben eine Größe von 350x350 Pixeln. Grauwertbilder haben einen Wertebereich von 0 bis 255 (falls nicht anders angegeben). Logische Operationen werden im Rahmen der Prüfung nur auf Binärbilder (Schwarz-Weiss-Bilder) angewendet. `true` wird durch den Wert 1 (=weiss) repräsentiert, `false` durch den Wert 0 (=schwarz).

Matlab Referenz

Notationen

Matrix $A = \begin{pmatrix} a & b \\ c & d \end{pmatrix}$ `A=[a b; c d];` *Spaltenvektor* $x = \begin{pmatrix} y \\ z \end{pmatrix}$ `x=[y;z]`

Zeilenvektor $e = \begin{pmatrix} f & g \end{pmatrix}$ `e=[f g]`

Command Reference

`D = bwdist(BW)`
computes the Euclidean distance transform of the binary image BW. For each pixel in BW, the distance transform assigns a number that is the **distance between that pixel and the nearest nonzero pixel** of BW. bwdist uses the Euclidean distance metric by default. D is the same size as BW.

`C=conv2(A,B)`
computes the two-dimensional convolution of matrices A and B.

`J = histeq(I,n)`
transforms the intensity image I, returning in J an intensity image with n discrete gray levels. A roughly equal number of pixels is mapped to each of the n levels in J, so that the histogram of J is approximately flat. (The histogram of J is flatter when n is much smaller than the number of discrete levels in I.) The default value for n is 64

`BW = im2bw(I,level)`
converts the intensity image I to black and white. The output binary image BW has values of 0 for all pixels in the input image with luminance g less than *level* and 1 for all other pixels:

$$bw = 0 \Leftrightarrow \frac{g - g_{min}}{g_{max} - g_{min}} < level$$

`IM2 = imclose(IM,SE)`
performs morphological closing on the grayscale or binary image IM, returning the closed image, IM2. The structuring element, SE, must be a single structuring element object.

`IM2 = imerode(IM,SE)`
erodes the grayscale, binary, or packed binary image IM, returning the eroded image IM2. The structuring element, SE, must be a single structuring element object.

`B = medfilt2(A)`
performs median filtering of the matrix A using the default 3-by-3 neighborhood.

`SE = strel('disk',R)`
creates a flat, disk-shaped structuring element, where R specifies the radius.

Grundlagen der Digitalen Bildverarbeitung LV 183.126		Datum: 7.12.2010
Mat.Nr.	Name	Studium

Folgende Liste enthält 10 Bildoperationen, die auf eines oder mehrere (z.B. $Y+Z$) der Bilder A-X angewandt wurden und eines der Bilder A-X als Ergebnis haben. Ihre Aufgabe ist die Rekonstruktion dieser 10 Bildoperationen. Tragen Sie bitte die Bildnamen (`A-X`) in die Kästchen ☐ der jeweiligen Operation ein. Jede korrekte Antwort wird mit einem Punkt belohnt. Für jene 4 Antworten, die den ersten vier verschiedenen Ziffern Ihrer Matrikelnummer entsprechen (sollten nur 3 verschiedene Ziffern auftreten, so wird durch "4" ergänzt), gibt es einen Punkt zusätzlich für eine korrekte Antwort und einen Abzugspunkt für eine falsche Antwort. Für entsprechend gute und korrekte Begründungen kann es Zusatzpunkte geben, die Verluste in anderen Abschnitten ausgleichen können!

0. ☐ `= medfilt2( ☐ );`

   Begründung: .....

1. ☐ `= conv2( ☐ ,[1 0 -1; 2 0 -2; 1 0 -1]);`

   Begründung: .....

2. ☐ `= histeq( ☐ );`

   Begründung: .....

3. ☐ `= 1-im2bw( ☐ ,100/255);`

   Begründung: .....

4. ☐ `= imerode( ☐ ,strel('disk',11));`

   Begründung: .....

5. ☐ `= imclose( ☐ ,strel('disk',30));`

   Begründung: .....

6. ☐ `= bwdist( ~ ☐ );`

   Begründung: .....

7. ☐ `= "Hough-Transform"( ☐ );`

   Begründung: .....

8. ☐ `= and( ☐ ,not( ☐ ));`

   Begründung: .....

9. ☐ `= or(im2bw( ☐ ,160/255),im2bw( ☐ ,160/255));`
   `% Verwenden Sie 3 verschiedene Bilder!`

   Begründung: .....

Grundlagen der Digitalen Bildverarbeitung LV 183.126		Datum: 7.12.2010
Mat.Nr.	Name	Studium

Binärbilder

A= 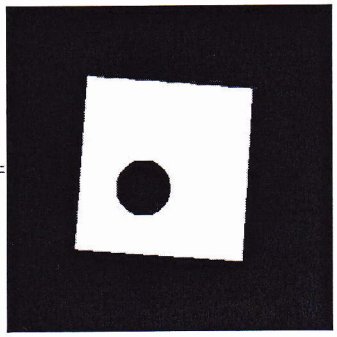

B= 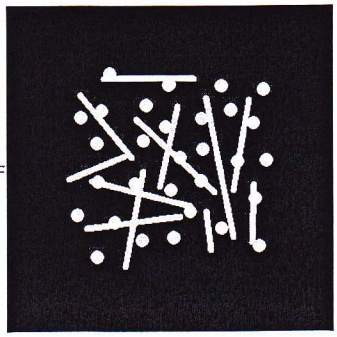

C= 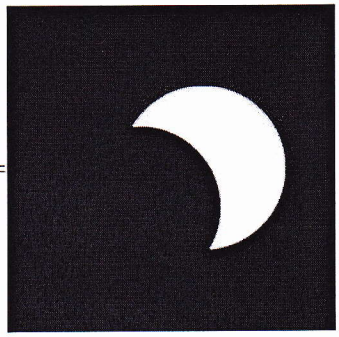

D= 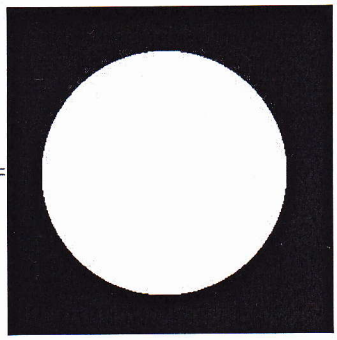

E= 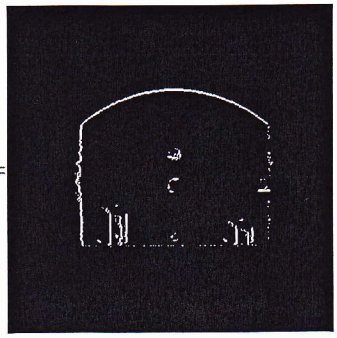

F= 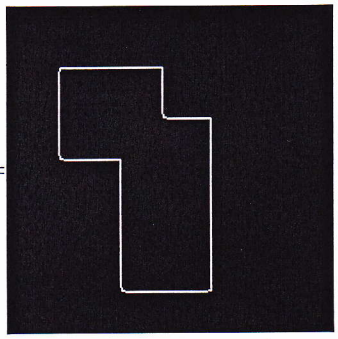

G= 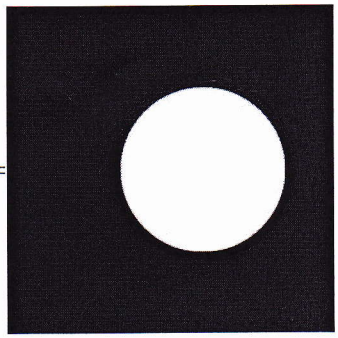

H= 

I= 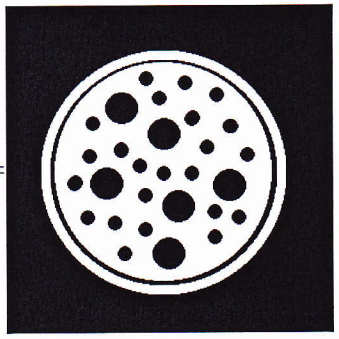

J= 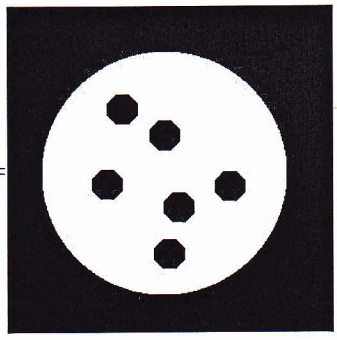

K= 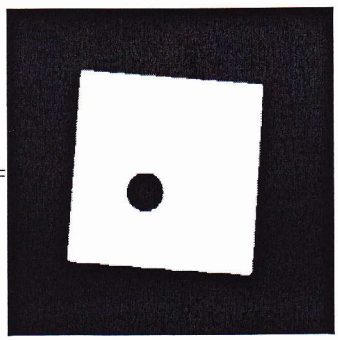

L= 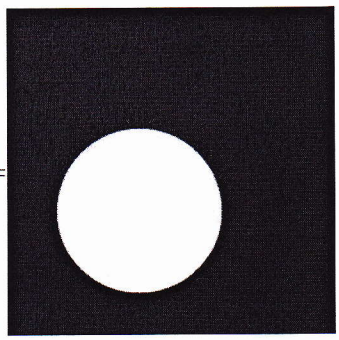

Grundlagen der Digitalen Bildverarbeitung LV 183.126		Datum: 7.12.2010
Mat.Nr.	Name	Studium

Grauwertbilder

M= 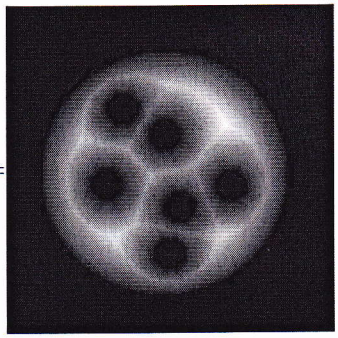

N= 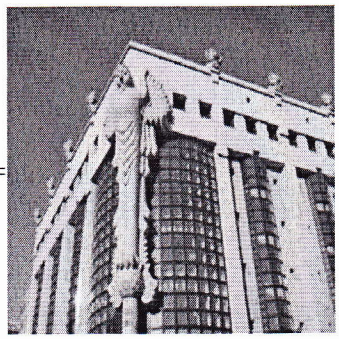

O= 

P= 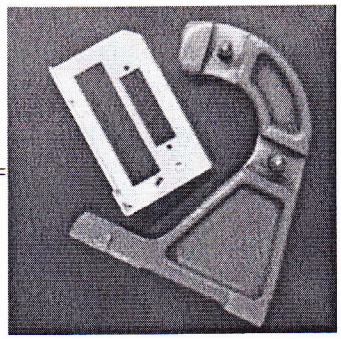

Q= 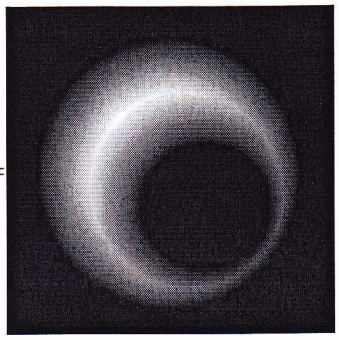

R= 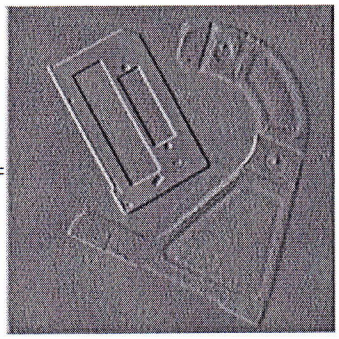

S= 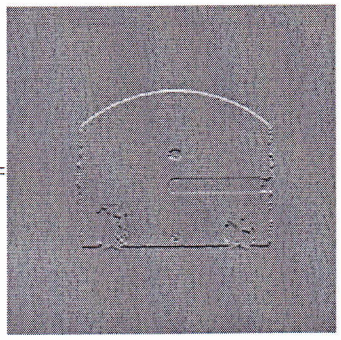

T= 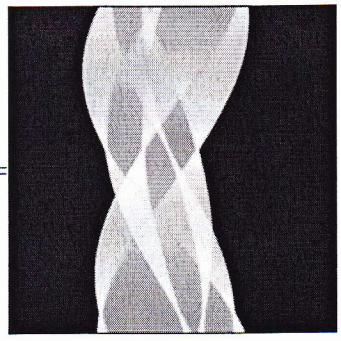

U= 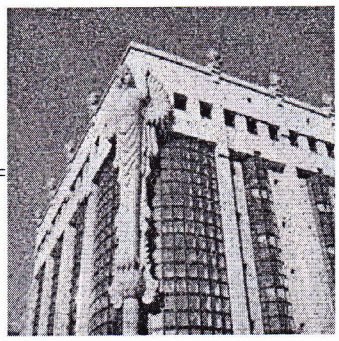

V= 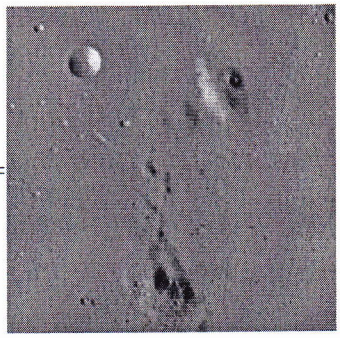

W= 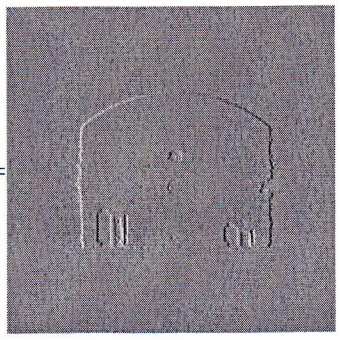

X= 

Grundlagen der Digitalen Bildverarbeitung LV 183.126		Datum: 7.12.2010
Mat.Nr.	Name	Studium

Teil II: Mathematisches Nachvollziehen (20)

In diesem Teil sollen Sie einfache Bildverarbeitungsoperationen numerisch nachvollziehen. Bezeichne $M_1, M_2, \ldots M_7$ die 7 Ziffern Ihrer Matrikelnummer M.

1 Rekonstruktion aus Kantenbildern (5)

1. Ein 4×4 Grauwertbild I wurde mit den zwei Filtern von Robert's Kantendetektor gefaltet: $G_x = \begin{pmatrix} 1 & 0 & 0 \\ 0 & \boxed{-1} & 0 \\ 0 & 0 & 0 \end{pmatrix} * I$; $G_y = \begin{pmatrix} 0 & 0 & 1 \\ 0 & \boxed{-1} & 0 \\ 0 & 0 & 0 \end{pmatrix} * I$. Für die Ränder wurde in beiden Fällen der zyklische Abschluß angenommen. Rekonstruieren Sie aus den 16 bekannten Werten alle restlichen 32 Werte von G_x, G_y, I.

2. In die mit ○ gekennzeichneten Pixel tragen Sie die 7 Ziffern Ihrer Matrikelnummer ein :

$G_x =$

0			○
	−1	○	
○		0	0

, $G_y =$

○			−1
		−1	
○	−1		2

, $I =$

○			8
		○	

.

3. Die speziellen Filter zerlegen $G_x(x, y)$ und $G_y(x, y)$ in 4 Teilklassen 0, 1, 2, 3, $\text{mod}(x + y, 4) =$ konst. und $\text{mod}(x - y, 4) =$ konst., die durch den zyklischen Abschluß und den jeweiligen Filter verknüpft sind, von einander aber unabhängig sind: Trage die Teilklassen in die folgenden Matrizen ein:

Klassen(G_x) =

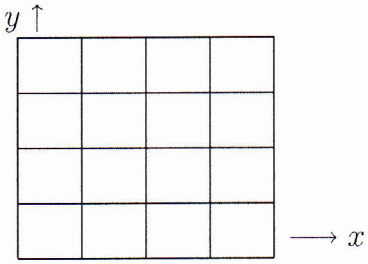

Klassen(G_y) =

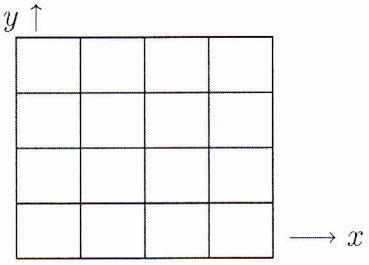

4. Der zyklische Abschluß und die Filter stellen eine Beziehung zwischen den vier Werten jeder Teilklassen von G_x und G_y her. Welche?

.....

.....

.....

2 RULI Chaincode (5)

1. Folgende Figuren 0 . . . 5 zeigen 6 geschlossene Kurven, die im Uhrzeigersinn durchlaufen werden:

0: 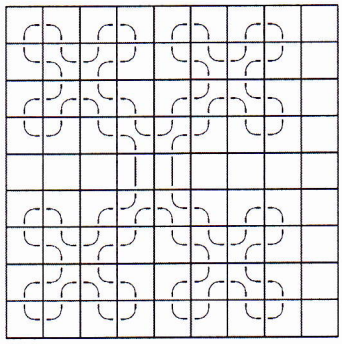

1: 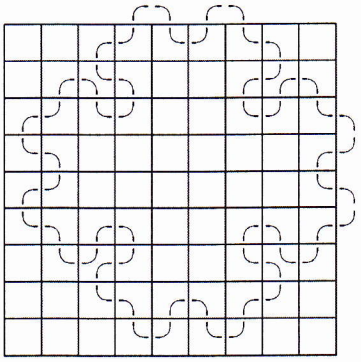

2: 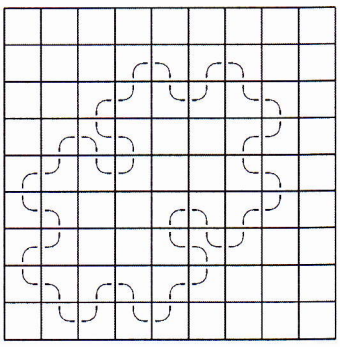

3: 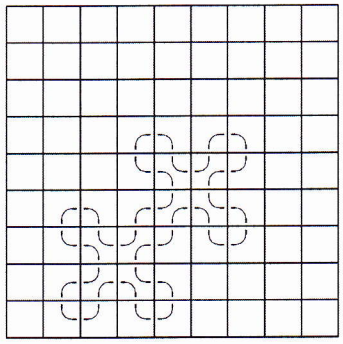

4: 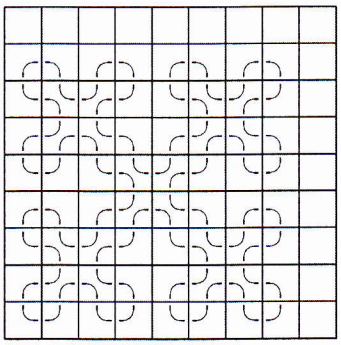

5: 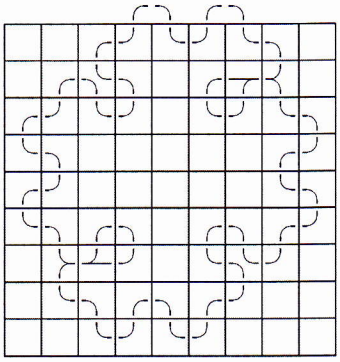

2. Bestimmen Sie die RULI Chain, die die Figur $\min\{M_7, 10 - M_7\} =$ ☐ erzeugt[1] und markieren Sie den Startpunkt:

   .....

3. Die folgenden Grammatiken $G = (\{R_n, L_n, I_n\}, \{S, R_i, L_i, I_i | 0 \leq i < n\}, S, P)$ erzeugen je eine Klasse von RULI Chains nach einer vorgegebenen Anzahl von Substitutionen n. Die Regel für das Startsymbol $S \rightarrow \cdots$ fehlt:

P_1 :	P_2 :
$R_{i-1} \rightarrow L_i R_i R_i;$	$R_{i-1} \rightarrow L_i R_i R_i R_i L_i;$
$L_{i-1} \rightarrow L_i;$	$L_{i-1} \rightarrow L_i R_i L_i;$
$I_{i-1} \rightarrow I_i;$	$I_{i-1} \rightarrow I_i.$

   Welcher Satz von Regeln kann die RULI-Kette aus 2. erzeugen? $\boxed{P_1}$ oder $\boxed{P_2}$

4. Begründung? .....

5. Zur Bestimmung der Startregel wenden Sie die Produktionsregeln zur Erkennung an, indem Sie die rechten Seiten einer Regel durch die linke Seite so lange ersetzen, bis die RULI Kette maximal 8 Codes lang ist:

   .....

   .....

   .....

6. Die fehlende Startregel müßte daher lauten: $S \rightarrow$ .....

[1] Klammern und Exponenten erlauben eine kompakte Schreibweise: $C^3 = CCC$, $(AB)^2 = ABAB$

3 Rekonstruktion aus Laplacepyramide (5 P)

1. Die Grundebene einer $2 \times 2/4$ Laplacepyramide wird als Distanztransformation von 8 mit 0 initialisierten Pixeln und der 8-Nachbarschaft bestimmt, 7 davon aus den Ziffern $M_i, i = 1, \ldots 7$. Tragen Sie 0 in Spalte M_i und der dem Wert entsprechenden Zeile von L_0 ein, alle anderen Elemente erhalten den minimalen 8-Abstand zu einem dieser Saatpixel.

2. Die Ebenen $L_1 = R(L_0)$ und $L_2 = R(L_1)$ werden aus der jeweilig darunter liegenden Ebene mit folgender Reduktionsfunktion bestimmt: $R\begin{pmatrix} a & b \\ c & d \end{pmatrix} = \left\lfloor \frac{a+b+c+d}{3} \right\rfloor$. Rationale Quotienten werden abgerundet.

	L_0							
Ziffer	7	M_1	M_2	M_3	M_4	M_5	M_6	M_7
0, 1								
2								
3								
4								
5								
6								
7	0							
8, 9								

$L_1 =$ 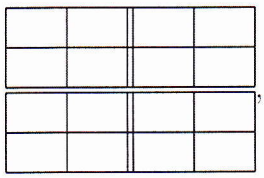 , $L_2 =$ 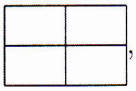 , $L_3 =$ 9

3. Diese 4 Ebenen bilden eine Laplace Pyramide, aus der Sie die zugrundeliegende Grauwertpyramide mit folgender Expansionsfunktion rekonstruieren: $E(g) = \begin{pmatrix} g-1 & g \\ g & g-1 \end{pmatrix}$.

$G_0 =$ 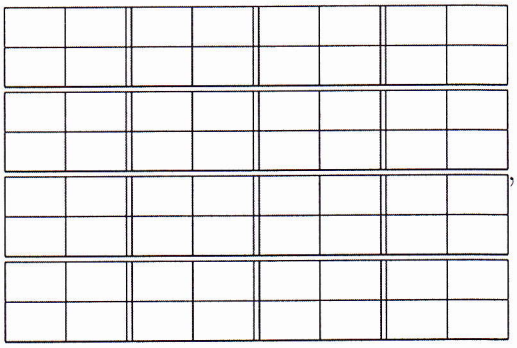 , $G_1 =$ 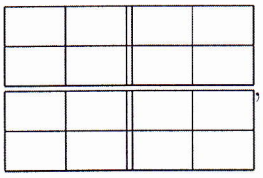 , $G_2 =$ 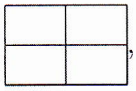 , $G_3 =$ 

Begründung: .....

.....

.....

.....

.....

Grundlagen der Digitalen Bildverarbeitung LV 183.126		Datum: 7.12.2010
Mat.Nr.	Name	Studium

4 Zwei Tetraeder (5)

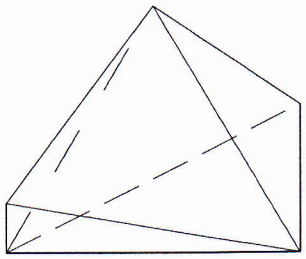

1. Zwei Tetraeder werden wie folgt zusammengelegt:
   Die 5 Eckpunkte, an denen mehr als 2 Tetraederflächen zusammentreffen, tragen die Ziffern M_1 bis M_5 Ihrer Matrikelnummer, M_6 wird in ein Tetraederdreieck eingetragen.

2. Ergänzen Sie die fehlenden Kanten (ohne Kreuzungen!) im RAG der Oberfläche der zwei Tetraeder.

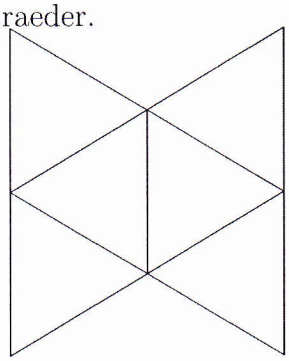

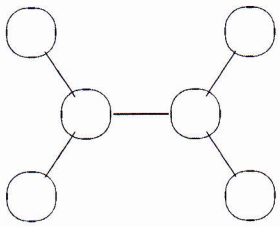

   Der vollständige RAG hat ☐ Knoten und ☐ Kanten.

3. Zeichnen Sie den dualen Graphen über den RAG.
   Der duale Graph hat ☐ Knoten und ☐ Kanten.

4. Übertragen Sie die Attribute M_1 bis M_6 in den Knoten des Region Adjacency Graphen (RAG) und die Knoten des dualen Graphen ein. Die restlichen Knoten des RAG sollen so gewählt werden, dass die Werte der Eckpunkte der Summe der Werte der angrenzenden Dreiecke entspricht.

5. Bestimme die Adjacency Matrix der Ziffern des RAG:

Ziffer	0	1	2	3	4	5	6	7	8	9	$\sum$
0											
1											
2											
3											
4											
5											
6											
7											
8											
9											

Grundlagen der Digitalen Bildverarbeitung LV 183.126		Datum: 7.12.2010
Mat.Nr.	Name	Studium

Grundlagen der Digitalen Bildverarbeitung LV 183.126		Datum: 7.12.2010
Mat.Nr.	Name	Studium

Teil III: Selektion von Literatur (16)

In Abschnitt 6 finden Sie 10 Titel wissenschaftlicher Publikationen. In Abschnitt 5 finden Sie 20 Literaturausschnitte (A-T) von denen Sie **12 diesen Titeln zuordnen müssen**. Einem Titel können somit mehrere Ausschnitte zugeordnet sein. Leider sind die Reihenfolge und die Zuordnungen, sowie einige Worte (markiert durch ...) der entsprechenden Beiträge verloren gegangen.

Je nach Wert der VORLETZTEN Ziffer M_6 Ihrer Matrikelnummer **streichen Sie 8 Literaturausschnitte in folgender Tabelle weg**:

M_6	Zu streichende Literaturausschnitte
0,1,2,3	A - H
4,5,6	G - N
7,8,9	M - T

Stellen Sie für die übrigen **12 Ausschnitte** die inhaltlichen Zuordnungen wieder her, indem Sie sie zu dem dazugehörenden Titel eintragen. Für eine korrekte Korrespondenz erhalten Sie 2 Punkte, für falsche und für fehlende Ausschnitte wird je 1 Punkt abgezogen. Maximal werden 16 Punkte gewertet.

5 Abstracts und Literaturausschnitte

A In a ... , the symmetric relationship is represented by undirected edges, while the asymmetric relationship is represented by directed edges. The asymmetric relationship is usually the conditional dependence between the samples (which incorporates weak class-specific information), while the symmetric relationship often measures the homogeneity (e.g., similarity) among the samples of a class. As a result, a ... incorporates two matrices that are associated to the directed subgraph and the undirected subgraph, respectively.

B This article introduces a method to determine in a robust manner the threshold in highly noisy gradient images. To enhance the robustness, the proposed technique is based on a piecewise linear regression to fit the whole descending slope of the histogram, rather than the search of some specific points. The algorithm gives a reliable estimation of the threshold, and is practically insensitive to the noise distribution, to the quantity of edge pixels to segment, and to random histogram fluctuations.

C To achieve these objectives, a novel minimization criterion is proposed. It consists of the minimization of the error between the descending slope of the histogram and its piecewise linear regression. It belongs to the histogram-based algorithms, but, unlike the main available methods, its computation relies on a wide portion of the histogram rather than a single bin or a few local bins. The technique is presented for gradient images, but can be generalized to other types of images. It does not rely on a specific graylevel unimodal distribution, but on the hypothesis of a less populated class belonging to the tail of the histogram.

D Since cameras blur the incoming light during measurement, different images of the same surface do not contain the same information about that surface. Thus, in general, corresponding points in multiple views of a scene have different image intensities. While multiple-view geometry constrains the locations of corresponding points, it does not give relationships between the signals at corresponding locations. This paper offers an elementary treatment of these relationships. We first develop the notion of ideal and real images, corresponding to, respectively, the raw incoming light and the measured signal. This framework separates the filtering and geometric aspects of imaging. We then consider how to synthesize one view of a surface from another; if the transformation between the two views is affine, it emerges that this is possible if and only if the singular values of the affine matrix are positive. Next, we consider how to combine the information in several views of a surface into a single output image. By developing a new tool called frequency segmentation, we show how this can be done despite not knowing the blurring kernel.

E We use segmentations to match images by shape. The new matching technique does not require point-to-point edge correspondence and is robust to small shape variations and spatial shifts. To address the unreliability of segmentations computed bottom-up, we give a closed form approximation to an average over all segmentations. Our method has many extensions, yielding new algorithms for tracking, object detection, segmentation, and edge-preserving smoothing. For segmentation, instead of a maximum a posteriori approach, we compute the central segmentation minimizing the average distance to all segmentations of an image. For smoothing, instead of smoothing images based on local structures, we smooth based on the global optimal image structures. Our methods for segmentation, smoothing, and object detection perform competitively, and we also show promising results in shape-based tracking.

F ... is important in several fields such as robotics, remote sensing, and imagery. The objective of this paper is to present several methods, ... We begin by reviewing the standard Hough transform (SHT), then three new methods are suggested: the revisited Hough transform (RHT), the parallel-axis transform (PAT), and the circle transform (CT). These transforms utilize a point-line duality to detect straight lines in an image. The RHT and the PAT should be faster than the SHT and the CT because they use line segments whereas the SHT uses sinusoids and CT uses circles. Moreover, the PAT, RHT, and CT use additions and multiplications whereas the SHT uses trigonometric functions (sine and cosine) for calculation. To compare the methods we analyze the distribution of the frequencies in the accumulators and observe the effect on the detection of false local maxima. We also compare the robustness to noise of the four transforms. Finally, an example with a real image is given.

G This paper introduced the formalism of the ideal image, consisting of the unblurred incoming light, and the real image, consisting of the blurred measured image. Because this framework separates the filtering and geometrical aspects, it makes it easy to derive several results. The notion of the ideal image might be useful for deriving other results. More formally, a relation between the outputs of filters applied at corresponding patches in different views was developed. This result was used to formulate and prove the accessibility theorem, which states the conditions under which, given two images of the same scene, one is accessible by the other (i.e., one image can be obtained by appropriately filtering the other). We then discussed the consequences of this result to the understanding of the space of all images of a scene. As an application of this framework, we showed that it is possible to perform multiple-view image reconstruction, even with an unknown blurring kernel, through the new tool of frequency segmentation.

H An image $\mathcal{I}$ is described by the Cartesian coordinates of its points. We denote by $\mathcal{H}$ the parameter space of coordinates (θ, ρ) associated with the lines. According to its definition, the SHT has the following properties:

Property 1. A point in an image $\mathcal{I}$ corresponds to a sinusoid in the parameter space $\mathcal{H}$.

Property 2. A point in the parameter space $\mathcal{H}$ corresponds to a line in the image $\mathcal{I}$.

Property 3. Points on a given line in an image $\mathcal{I}$ define sinusoids in the parameter space $\mathcal{H}$ which intersect at the same point.

Property 4. Points on a given sinusoid in the parameter space $\mathcal{H}$ correspond to lines in the image $\mathcal{I}$ which intersect at the same point.

I The shape of an object (as conveyed by edge curves) is among its most distinctive features. Though a category of objects can vary greatly in appearance as the illumination or coloring changes, the overall shape of the objects can be relatively invariant. People can easily recognize objects just from their shapes, and applying shape for matching and recognition has been an important topic in computer vision.

J Data in a paper document are usually captured by optical scanning and stored in a file of picture elements, called pixels, that are sampled in a grid pattern throughout the document. These pixels may have values: OFF (0) or ON (1) for binary images, 0 255 for gray-scale images, and 3 channels of 0255 colour values for colour images. At a typical sampling resolution of 120 pixels per centimetre, a 20 x 30 cm page would yield an image of 2400x3600 pixels. When the document is on a different medium such as microfilm, palm leaves, or fabric, photographic methods are often used to capture images. In any case, it is important to understand that the image of the document contains only raw data that must be further analysed to glean the information.

K The ... operator-based edge detectors localize edges with the zero-crossings of the high-frequency components of image. One problem arising from this is that the noise contained in the high-frequency components will yield false zero-crossings. Noting that the amplitudes of high-frequency components of edges are relatively larger than that of noise, we may remove the low amplitudes of noise by thresholding the high-frequency components of an image.

L Segmentation occurs on two levels. On the first level, if the document contains both text and graphics, these are separated for subsequent processing by different methods (Wong 1982; Fletcher 1988; Jain 1992). On the second level, segmentation is performed on text by locating columns, paragraphs, words, and characters; and on graphics, segmentation usually includes separating symbol and line components. For instance, in a page containing text and some illustrations similar to the pages of this journal, text and graphics are first separated. Then the text is separated into its components down to individual characters. The graphics is separated into its components such as rectangles, circles, connecting lines, symbols etc. After this step an image is typically broken down into its basic components such as an individual character or a graphical element.

M Major differences exist between the moment approach to curve parameterization and the various Hough-transformtype methods. One important difference is that the moment approach uses no accumulator array and overall requires very little memory. Another is that the moment method does not depend on the sharpness or smoothness of edges and no edge-detection preprocessing step is necessary. (However, other types of preprocessing that reduce noise or otherwise simplify the image may be of use. Some examples are given in Section 5.) Still another point of distinction between our method and much previous work is that ours offers a unified treatment for all types of conics (circles, parabolas, etc.). However, perhaps a more fundamental difference is philosophical in nature, as the following example shows.

N The vertices of a ... represent the samples, e.g., superpixels of an image. The vertices are connected by directed edges and/or undirected ones. A directed edge represents the dependence between the vertices that it connects (which is asymmetric), while an undirected edge represents the similarity between the vertices (which is symmetric). The directed and the undirected subgraphs represent our weak top-down and trustworthy bottom-up priors, respectively. Then, an image is segmented by classifying the vertices of the hybrid graph into two clusters, with one cluster being the foreground containing object(s) of the class and another being the background.

O Characteristically, many attempts to implement Blum's original definition in the discrete world failed to preserve such fundamental properties as connectivity or Euclidean metrics. Basically, we can distinguish between four substantially different variants of skeletonization algorithms:

(1) simulation of the 'grassfire';

(2) analytical computation of the medial axis;

(3) topological thinning; and

(4) medial axis extraction from a distance map.

P Typically, the geometric similarity between two shapes is a measure of how well the primitives forming the shapes and / or their spatial organizations agree [919]. Tree data structure has been widely used for describing shapes,as it provides a natural representation of the inclusion relations of the primitives.When a shape (primitives and their inclusion relations)is represented by a tree,the best correspondence between two given shapes can be expressed as the best partial match between their trees.Accordingly, the shape dissimilarity is computed as the edit distance which is defined as the cost of transforming the first tree into the second one by using node removal, node insertion and attribute change operations [20]. In the shape literature, it is an accepted practice to form tree or graph descriptions using shape skeletons, and to match these descriptions using edit distance [12,13,15,16,21]. Typically, these works are generic and they ignore contextual effects,despite the observation that human dissimilarity judgements are biased by the other shapes [5,6,8,22,23,24].

Q Interest in computing parametric descriptions of lines and conics in images has been rekindled by new image coding schemes based on approximating images with geometrical elements such as wedgelets and curvelets [8], [31], [23] and by the opportunity to reduce ringing artifacts in compressed images [28]. For such applications, resistance to noise, computational speed, and memory requirements are major concerns. Moment-based techniques have long been recognized as well suited in this context, and an extensive body of theoretical and computational results has been developed.

R This edge-matching filter should also make the value of the output noise variance σ_0^2 as small as possible. Similar to Canneys work [2], we define the criterion ρ as the improvement of signal-to-noise ratio from input to output at the location $n = 0$, where

$$\rho = \frac{h(0)}{\sum_{n=-N}^{N} h^2(N)} \tag{1}$$

S Skeletal trees are commonly used in order to express geometric properties of the shape. Accordingly, tree-edit distance is used to compute a dissimilarity between two given shapes.We present a new tree-edit based shape matching method which uses a recent coarse skeleton representation. The coarse skeleton representation allows us to represent both shapes and shape categories in the form of depth-1 trees. Consequently,we can easily integrate the influence of the categories in to shape dissimilarity measurements. The new dissimilarity measure gives a better within group versus between group separation, and it mimics the asymmetric nature of human similarity judgements.

T Robust and time-efficient skeletonization of a (planar) shape, which is connectivity preserving and based on Euclidean metrics, can be achieved by first regularizing the Voronoi diagram (VD) of a shape's boundary points, i.e. by removal of noise-sensitive parts of the tessellation and then by establishing a hierarchic organization of skeleton constituents. Each component of the VD is attributed with a measure of prominence which exhibits the expected invariance under geometric transformations and noise. The second processing step, a hierarchic clustering of skeleton branches, leads to a multiresolution representation of the skeleton, termed skeleton pyramid.

6 Welche Ausschnitte gehören zu folgenden Titel ?

0 Old and new straight-line detectors: Description and comparison

Ausschnitt(e): .....

Begründung(en): .....

1 Document image analysis: A primer

Ausschnitt(e): .....

Begründung(en): .....

2 Hierarchic Voronoi skeletons

Ausschnitt(e): .....

Begründung(en): .....

3 Robust threshold estimation for images with unimodal histograms

Ausschnitt(e): .....

Begründung(en): .....

4 Laplacian Operator-Based Edge Detectors

Ausschnitt(e): .....

Begründung(en): .....

5 Unsupervised Object Segmentation with a Hybrid Graph Model (HGM)

Ausschnitt(e): .....

Begründung(en): .....

6 Rigid Shape Matching by Segmentation Averaging

Ausschnitt(e): .....

Begründung(en): .....

7 Dissimilarity between two skeletal trees in a context

Ausschnitt(e): .....

Begründung(en): .....

8 Curve Parameterization by Moments

Ausschnitt(e): .....

Begründung(en): .....

9 Image Transformations and Blurring

Ausschnitt(e): .....

Begründung(en): .....